1-6-2015

Functional Layer-By-Layer Design of Xerogel-Based 1st Generation Amperometric Glucose Biosensors

Nicholas G. Poulos

Jackson R. Hall

Michael C. Leopold
University of Richmond, mleopold@richmond.edu

Recommended Citation

N. Poulos, J. Hall, and M.C. Leopold, "Functional Layer-By-Layer Design of Xerogel-Based 1st Generation Amperometric Glucose Biosensors," *Langmuir* 2015, *31*(4), 1547-1555.

For submission to Langmuir

Functional Layer-By-Layer Design of Xerogel-Based 1st Generation Amperometric Glucose Biosensors

Nicholas G. Poulos, Jackson R. Hall, and Michael C. Leopold*

Department of Chemistry, Gottwald Center for the Sciences,
University of Richmond, Richmond, VA 23173

ABSTRACT

Xerogel-based 1st generation amperometric glucose biosensors, constructed through specific layer-by-layer assembly of films featuring glucose oxidase doped xerogel, a diffusion-limiting xerogel layer, and capped with both electropolymerized poly-phenol and blended polyurethane semi-permeable membranes, are presented. The specific combination of xerogels formed from specific silane precursors, including propyl-trimethoxy silane, isobutyl-trimethoxy silane, octyl-trimethoxy silane, and hydroxymethyl-triethoxy silane, exhibit impressive dynamic and linear ranges of detection (e.g., ≥24-28 mM glucose), low response times, as well as significant discrimination against common interferent species such as acetaminophen, ascorbic acid, sodium nitrite, oxalic acid and uric acid as determined by selectivity coefficients. Additionally, systematic electrochemical and contact angle studies of different xerogel silane precursors, varying in structure, chain length and/or functional group, reveal that sensor performance is more dependent on the tunable porosity/permeability of the layered interfaces rather than the hydrophobic character or functional groups within the films. While the sensing performance largely exceeds that of existing electrochemical glucose sensing schemes in the literature, the presented layered approach establishes the specific functionality of each layer working in concert with each other and suggests that the strategy may be readily adaptable to other clinically relevant targets and is amenable to miniaturization for eventual *in situ* or *in vivo* sensing.

* To whom correspondence should be addressed. Email: mleopold@richmond.edu. Phone: (804) 287-6329. Fax: (804) 287-1897

■ INTRODUCTION

Research examining the materials and mechanisms related to the development of highly functional biosensor strategies continues to be of significant interest to the scientific community as the potential need for applications of such devices continues to expand, particularly in the areas of medicine, food industry, and environmental testing/monitoring.[1-3] The study of electrochemical biosensors remains a major facet of this work as they represent relatively simple strategies that, compared to their spectroscopy-based counterparts, are inexpensive and much more amenable to *in vitro* remote sensing and/or *in vivo* usage as implantable microelectrode devices. Summarized in a review by Wang,[1] much attention has been devoted over the years to the development of electrochemical glucose biosensors not only as a response to the growing diabetes epidemic but also because it represents a fundamentally robust model system for investigating other aspects of electrochemical biosensor design.

First generation amperometric glucose biosensors remain as one of the more popular electrochemical strategies applied to developing biosensing research and technology. In most cases, these systems rely on immobilized enzyme (e.g., glucose oxidase, GOx) interacting with the analyte (e.g., glucose) in an enzymatic reaction that produces H_2O_2, a by-product subsequently oxidized at an electrode in proportion to the amount of glucose present in the solution. While still dependent on efficient diffusion and oxidation of the H_2O_2 at a working electrode, 1st generation schemes are non-mediated and utilize only one type of enzyme, unlike 2nd and 3rd generation biosensors, respectively.[1] It follows then that enzymatic activity and stability at the electrode surface through effective immobilization is a critical aspect to achieve sufficient signal-to-noise ratio in 1st generation biosensor designs.

While many enzyme immobilization strategies have been studied (e.g., electropolymerization,[4] nano-porous gold,[5] hydrogels,[6] microgels,[7] self-assembled monolayers,[8] nanoparticle film assemblies[9]), sol-gel matrices persist as particularly interesting scaffold as they are able to be formed under mild conditions, maintain enzyme structure/activity, as well as exhibiting chemical inertness, mechanical rigidity/stability, and negligible swelling with immersion in sample solutions.[10] A seminal report[11] by Bright and coworkers in 1994 examined the use of sol-gel materials as a functional

component to a glucose biosensor, illustrating a layer-by-layer (L-B-L) assembled sensor design where GOx is "sandwiched" between two sol-gel layers. Shortly thereafter, work by Pandey et al. used a similar layered, sandwich configuration in a number of reports focused on organically-modified sol-gel structures to create sol-gel based glucose biosensors.[12,13] These early reports established both the viability of sol-gel materials in electrochemical biosenors as well as the criteria for which to evaluate the sensors, including sensitivity, limit-of-detection, linear/dynamic range, response time, inteferent exclusion, and stability.

More recently, "sandwich configurations" utilizing sol-gels have morphed into L-B-L approaches targeting an expanding array of analytes where the sol-gel is impregnated with enzyme including, for example, sol-gel based sensors for cholesterol and lactate developed by Vagin et al. and Karyakin et al., respectively.[14, 15] In terms of glucose sensors, Schoenfisch and coworkers have elegantly refined the L-B-L approach for biosensor design by marrying the xerogels with semi-permeable membranes and biocompatibility advances to progress toward needle type implantable devices with demonstrated *in vivo* capability.[16,17] Another growing trend over the last decade has been the embedding of nanomaterials (NMs) into the sol-gel layers of a layered sensing scheme,[18,19] including metallic nanoparticles[20] as well as carbon-based materials (e.g., carbon nanotubes[21]) - the most notable advantage being an increase in sensor sensitivity. Aside from increasing the complexity, cost, and materials needed, a major disadvantage of incorporating NMs into a biosensor scheme is some loss of versatility, as each sensor has been intricately designed for only one analyte. The presence of NMs, while enhancing the analytical signal, is also likely to increase the sensor's response to common inteferent species.[22] In this respect, a facile L-B-L strategy for constructing biosensors without NMs but with the potential versatility of adaptation to other analyte species would be of high interest, particularly if there is no significant sacrifice of performance and viability for *in vitro* or *in vivo* development is maintained.

In this work, we present a robust and functional L-B-L strategy for the construction of a high performance 1st generation amperometric glucose biosensor utilizing a combination of enzyme-doped and un-doped xerogel layers and semi-permeable membranes, each layer serving a specific function in concert with each other.

These films exhibit excellent sensing performance compared to other strategies with particularly large linear ranges of step response and very effective interferent discrimination aspects. The study also establishes the dependence of sensor performance on xerogel structure via manipulation of the silane precursor. While many reports tout the tunable porosity of sol-gel materials as an advantage of their use for enzyme encapsulation,[10] few reports actually seize on this aspect of the material and demonstrate its effect on the signal. To our knowledge, a systematic elaboration of these structure-function relationships is lacking in the literature, expanding the scope of the study beyond the simple presentation of another sensing scheme to a greater fundamental understanding of L-B-L approaches, including exploration of both xerogels and semi-permeable materials and their potential adaptation to other clinically relevant targets.

■ EXPERIMENTAL DETAILS

Materials and Instrumentation. All chemicals were purchased from Sigma-Aldrich unless specifically stated. Tecoflex SG-80A polyurethane (TPU) was obtained from Lubrizol and Hydrothane AL25-80A polyurethane (HPU) was obtained from AdvanSource Biomaterials. All solutions were prepared using 18.2 MΩ ultra-purified water. Amperometric current-time (I-*t*) curves, recorded with an 8-channel potentiostat (CH Instruments, 1000B), were used to evaluate the analytical performance of the sensors as described below. Electrochemical cells were composed of modified platinum working electrodes (2 mm diameter), a common Ag/AgCl (saturated KCl) reference electrode (CH Instruments), and a common platinum wire counter electrode (Sigma-Aldrich). Silanes used for fabricating xerogels, purchased from Sigma-Aldrich or Gelest, were stored in a desiccated glove box (Plas Laboratories, Inc.) and eventually transferred using sealed micro-centrifuge to maintain the dry, N_2 environment and eventually used/deposited in a relative humidity (RH) controlled chamber (Cole-Parmer). Contact angle measurements were made with a Rame-Hart 300 goniometer affixed with a nitrogen-purged environmental chamber using 10 μL drops of ultra-purified water.

Preparation of Sol-Gel Biosensors. Platinum working electrodes were polished successively with 1.0, 0.3, and 0.05 μm Al_2O_3 powder (Electron Microscopy Sciences)

before electrochemical cleaning via cycling in 0.1 M H_2SO_4 between +1.2 V and -0.25 V at 0.25 V/s until the voltammetry was characteristic of a clean platinum surface.

For fabrication of the biosensor, two microcentrifuge tubes, one with 9 mg of glucose oxidase (GOx) dissolved in 75 μL of water and the other containing 25 μL of silane mixed with 100 μL of tetrahydrofuran (THF), were shaken on a vortex (10 min.) inside a humidity-controlled chamber (50% RH). GOx solution (50 μL) was added to the silane/THF mixture followed by another 10 min. of vortex agitation. A 3 μL aliquot of the final sol-gel mixture was deposited on the platinum electrode and allowed to dry at 50% RH for ~4 minutes. A second layer of sol-gel (diffusion-limiting layer), prepared in the same manner as described above without adding GOx, was deposited on top of the first sol-gel layer. The sol-gels were then allowed to age at 50% RH for 48 hours to form xerogels.[22] Note: The environment during aging is critically important as sensor performance has been shown to vary drastically depending on time and RH.[22] The specific silanes used in this study to create individual sol-gels included methyl-trimethoxy silane (MTMS), propyl-trimethoxy silane (PTMS), octyl-trimethoxy silane (OTMS), octadecyl-trimethoxy silane (ODTMS), 3-mecaptopropyl-trimethoxy silane (MPTMS), isobutyl-trimethoxy silane (IBTMS), phenyl-trimethoxy silane (PhTMS), aminopropyl-trimethoxy silane (APTMS), hydroxymethyl-triethoxy silane (HMTES), and 11-mercaptoundecyl trimethoxy silane (11-MUDTMS).

For application of the poly-phenol (PP) selective membrane, a previously reported preparation was adapted.[16, 23, 24] In brief, xerogel-modified electrodes were immersed in 25 mL of a 0.04 M phenol solution (4.4 mM potassium phosphate buffer (PBS) at pH 7, degassed with N_2 for 20 minutes). Electropolymerization of phenol was employed using chronocoulometry, holding the potential of the working electrode at +0.9 V (vs. Ag/AgCl, satrd. KCl) for 900 seconds. The PP/xerogel-coated electrodes were rinsed with PBS and allowed to dry (30 min.).

The outer polyurethane (PU) blended semi-permeable membrane was applied as previously reported.[16,22] For glucose sensing materials, for example, the PU blend was prepared from a 50:50 mixture of 50 mg of both HPU and TPU dissolved in 2.5 mL of ethanol and THF, respectively, that was stirred overnight. A 10.0 mL aliquot of the PU

blend was then deposited on the dry electrode and allowed to dry (30 min.) to complete the composite film biosensor.

Evaluation of Glucose Biosensor Performance. As in prior work,[16, 22] sensors were soaked in PBS (4.4 mM; pH 7) for 1 hour prior to testing to ensure solution saturation into the xerogel materials. For biosensing performance, assembled sensors were immersed in 25 mL of stirring PBS (4.4 mM; pH 7) for current-time (I-*t*) experiments where the working electrode potential was held at +0.65 V (vs. Ag/AgCl, satrd. KCl) for 20 minutes before successive 25 μL injections of 1 M glucose solution at 100 sec. intervals. Sensor sensitivity to glucose was based off of linear regression analysis of calibration curves for sensor current response at increasing glucose concentrations. A conservative definition of response time ($t_{R\text{-}95\%}$), seconds until 95% of total current response recorded, was employed.[16,22] As previously described in biosensing literature, amperometric selectivity coefficients (K^{amp}) were used to evaluate interferent responses and were calculated using the following equation:

$$K^{amp}_{Glucose,\ j} = \log\left(\frac{\Delta I_j / C_j}{\Delta I_{Glucose} / C_{Glucose}}\right)$$

where ΔI_j and $\Delta I_{glucose}$ are the measured currents for a specific interferent species (j) and glucose at concentrations of C_j and $C_{glucose}$, respectively.[16,22,25] If necessary, sensors were stored at 5-7° C immersed in PBS (4.4 mM; pH 7).

■ RESULTS AND DISCUSSION

Layered-Xerogel Biosensor Assembly and Performance. Our layered xerogel-based 1st generation glucose biosensor model is depicted in **Figure 1** and features several functional layers in a "sandwich" configuration scheme that exhibit highly effective sensing performance. As described in the Experimental Section, fabrication involves layer-by-layer (LBL) modification of a platinum working electrode with an initial enzyme-doped xerogel layer that is immediately followed with a second, diffusion-limiting xerogel not embedded with enzyme. The xerogels are formed from typical sol-gel chemistry under controlled conditions as previously demonstrated in our laboratory[22]

and by others.[16] The xerogel layers are topped with two additional layers for additional selectivity and interferent discrimination: a poly-phenol (PP) layer formed from the electropolymerization of phenol to form an inner-selective membrane and a final interfacial layer, the outer selective membrane, of polyurethane (PU) blend that has been shown to reduce interferent response in other sensing schemes.[16]

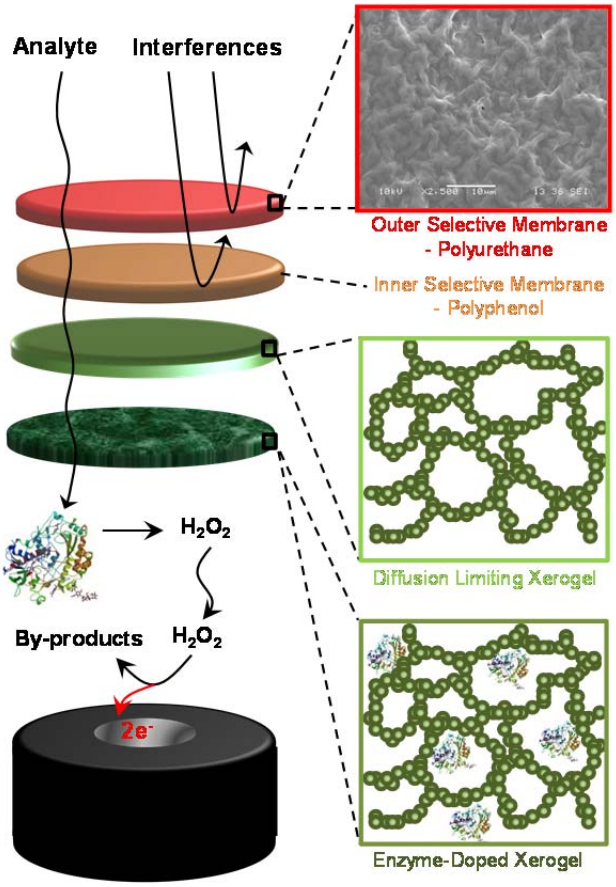

Figure 1. Schematic of layered strategy of xerogel-based, 1st generation amperometric glucose biosensor featuring an enzyme-doped and diffusion-limiting xerogel layers and capped with semi-permeable electropolymerized poly-phenol and polyurethane outer membranes.

This specific combination of layers yields a composite film material that acts as a effective 1st generation biosensor with tunable properties. Biosensor performance for this model system is highlighted by an extensive linear/dynamic range, fast response time, as well as, excellent sensitivity/selectivity and stability. **Figure 2** illustrates a typical amperometric current-time (I-*t*) curve during successive glucose injections (1 mM) at a propyl-trimethoxy silane (PTMS) biosensor. Well-defined stair-step responses between 0 and 30 mM translated to a highly linear calibration curve will a large linear range (Fig. 2A, inset), a notable attribute of the performance of these particular systems

compared to other schemes. The performance attributes of the PTMS-layered xerogel system developed here are summarized in **Table 1** and compared to other reported amperometric glucose sensors in the literature within the Supporting Information (Table SM-1). The response time for PTMS, approximately 16 seconds, is defined as the time it takes to achieve 95% of the final amperometric signal upon injection. We note that it is the specific

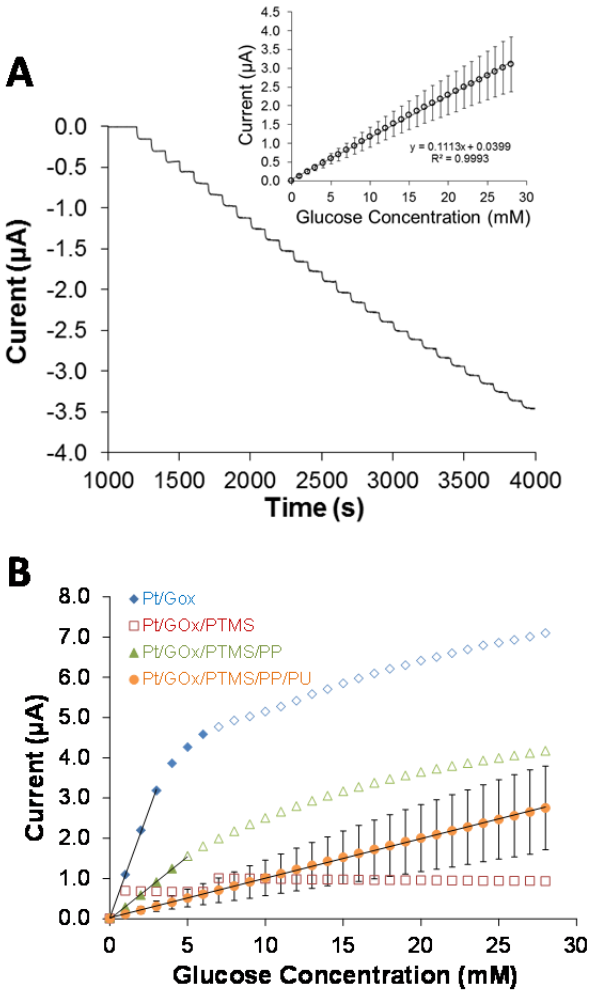

Figure 2. (A) Amperometric *I-t* curve and corresponding calibration curve (**Inset**) during successive 1 mM injections of glucose at a platinum electrode modified with GOx-doped PTMS xerogel, un-doped PTMS xerogel, poly-phenol (PP), and polyurethane layers (PU) and; **(B)** glucose calibration curves from control experiments of at the various stages of L-B-L construction of the xerogel-based sensor. Solid symbols indicate a step like response whereas open symbols indicate a non-step response (dynamic range). Linear regression is performed for linear step-responses (linear range). In some cases, error bars were intentionally not included for clarity.

combination and order in the L-B-L approach here enables the observed effective biosensing performance. Layered PTMS control systems tested without the selective membranes and/or diffusion-limiting xerogel layers yielded calibration curves featuring extremely high sensitivity (only at concentrations below 4 mM) and severely limited step response and linear ranges (**Figure 2B**). Only the specific combination of the doped and

un-doped PTMS-layered xerogel capped with both PP and PU ensured effective performance of the sensor.

A significant challenge of most biosensor designs is achieving sufficient sensitivity while simultaneously discriminating against common interferent species. For example, recent activity in this field has explored the use of nanomaterials (NMs) as a means of enhancing amperometric signal from the analyte.[3, 18, 19] Unfortunately, in many cases, the use of the NMs also enhances the signal from common interferents that are either found endogenously (e.g., ascorbic acid, uric acid) or are introduced to the physiological system.[22] In this latter regard, acetaminophen remains a challenging interferent to negate in most sensing schemes. The low oxidation potential of acetaminophen makes it electroactive during most amperometric measurements of H_2O_2. Additionally, it will be present as an interferent in many clinical applications where *in vivo* or *in vitro* sensing would have the most impact, either self-administered or prescribed by medical staff.[1] One of the real strengths of this layered xerogel scheme appears to be maintaining effective sensitivity while exhibiting comparatively low response to interferents. By itself, PP has been shown extremely effective at excluding common and relevant interferent species at both a bare electrode (Supporting Information) and xerogel-based biosensing schemes.[16] Similarly, blended PU layers are established semi-permeable membranes.[16] **Figure 3A** shows a typical I-*t* curve of a PTMS xerogel system capped with both PP and PU during injections of common interferents (acetaminophen, ascorbic acid, sodium nitrite, oxalic acid, and uric acid) as well as glucose injections of different concentrations. Current responses for the interferents are nearly negligible compared to that of the glucose injections, indicating excellent discriminatory selectivity of the sensing scheme.

Selectivity coefficients (K^{amp}), calculated as described in the Experimental Details, for each injected species are graphically displayed in **Figure 3B** to illustrate the changing selectivity during L-B-L construction of the sensor. As shown, uncapped xerogel layers (i.e., without PP or PU), Fig. 3B-a, only discriminate against oxalic acid and sodium nitrite (negative K^{amp} values). With the addition subsequent layers of PP and PU layers (Fig. 3B-b and 3B-c), signal from all interferents is suppressed while the glucose signal is still readily observable. The actual K^{amp} values for the different layers

are included as part of an extensive table contained in the Supporting Information and provide a quantitative measure of interferent discrimination that exceeds most reports for the selective detection of glucose via biosensing devices of this nature.[16, 22, 25] We note that, as evidenced by the I-*t* curves and interferent tracking (Fig. 3), sensitivity toward glucose is sacrificed to a small degree in exchange for greater selectivity through interferent discrimination and a more well-defined step response for glucose. Lower

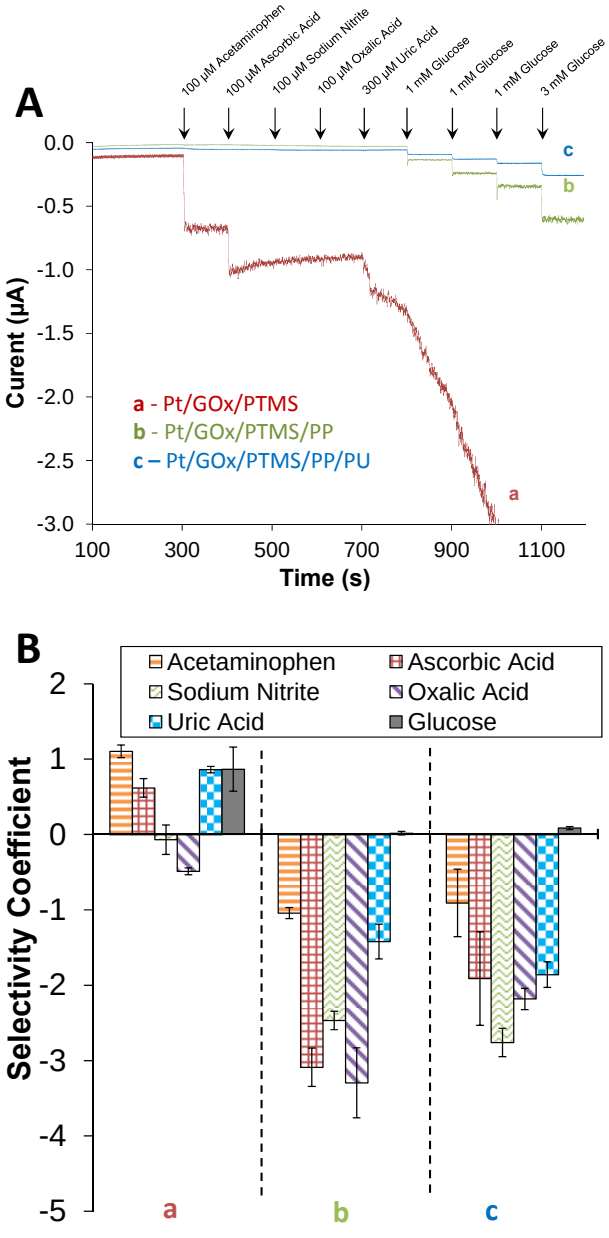

Figure 3. **(A)** Amperometric *I-t* curves and **(B)** selectivity coefficients for successive injections of common interferent species (100 µM) and glucose (1 mM and/or 3 mM) at a platinum electrode modified with various stages of L-B-L construction including **(a)** GOx-doped PTMS xerogel and un-doped PTMS xerogel with **(b)** poly-phenol (PP) or with **(c)** poly-phenol and polyurethane (PU) capping layers. Note: Uric acid was tested at 300 µM.

current signals for glucose are still readily detected with low limit-of-detection values (Table 1) while interferent responses are essentially negligible.

The PTMS-layered xerogel biosensors exhibited very good stability in terms of both maintaining sensitivity, selectivity, and response time during storage. As seen in **Figure 4**, sensors stored in PBS (5-7°C) and tested periodically over the course of at least two weeks, showed only modest degradation in terms of sensitivity and response time (Fig. 4A). With the exception of uric acid, selectivity coefficients for common interferents were stable or improved over the two-week time period (Fig. 4B). Sensors were specifically monitored over a two week period since their development is eventually intended for short-term clinical uses (e.g., emergency room, intensive care, maternity ward). The PTMS-layered xerogel system was tested out to 21 days and maintained a relatively low response time and only exhibited an additional 10% drop in sensitivity over the extra week.

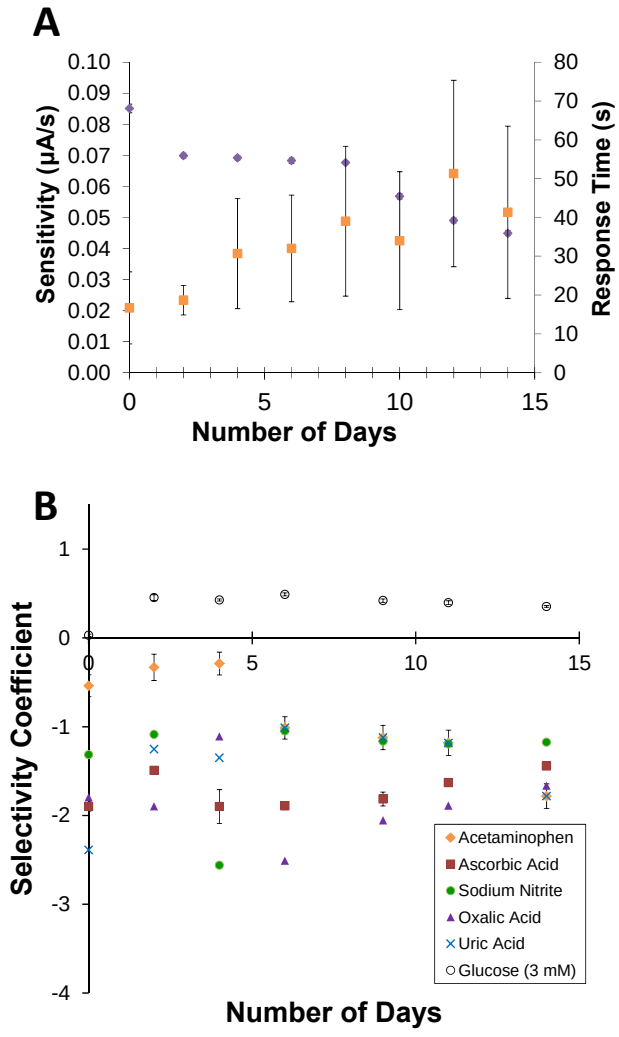

Figure 4. (A) Stability tests for layered PTMS xerogel glucose biosensors for sensitivity (♦) and response time (■) as well as **(B)** the selectivity coefficients of common interferents and glucose (3 mM) monitored over a two week period. Sensors were stored at 4-7°C immersed in PBS (pH 7; 4.4 mM) Note: In some cases, error bars are smaller than markers for average sensitivity

Layered-Xerogel Biosensing Dependence on Silane Precursor. Aside from excellent sensing performance, the layered-xerogel design, via manipulation of the silane used to form the xerogel layers, readily allows for significant tuning of the sensitivity without sacrificing impressive step-response, linear range, or interferent discrimination. The general structure of the silane used for the xerogels is R-trimethoxy silane. **Scheme I** illustrates a variety of commercially available silane compounds. The silanes can be categorized by their R group, varying in chain length (**1a-1d**): including methyl-trimethoxy silane (MTMS, **1a**), propyl-trimethoxy silane (PTMS, **1b**), octyl-trimethoxy silane (OTMS, **1c**), and octadecyl-trimethoxy silane (ODTMS, **1d**); or functional group (**2-6**): 3-mecaptopropyl-trimethoxy silane (MPTMS, **2**), isobutyl-trimethoxy silane (IBTMS, **3**), phenyl-trimethoxy silane (PhTMS, **4**), aminopropyl-trimethoxy silane (APTMS, **5**), hydroxymethyl-triethoxy silane (HMTES, **6**), and 11-mercaptoundecyl trimethoxy silane (11-MUDTMS, not pictured). **Figure 5A** shows typical calibration curves of layered xerogel sensors where the chain length of the silane precursor R group

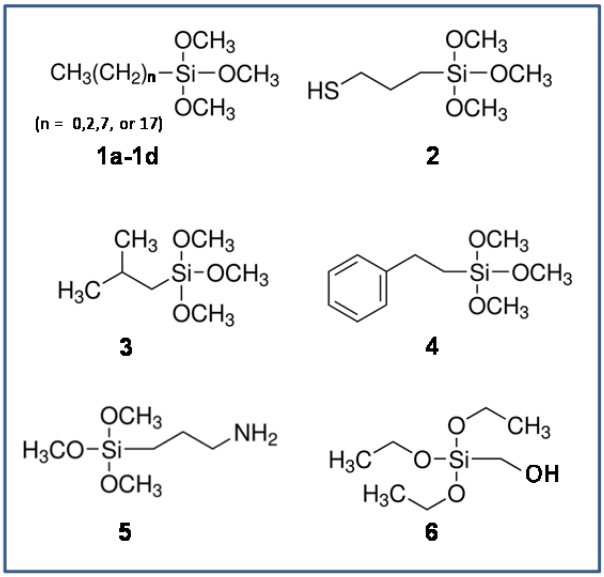

Scheme I

was varied from methyl to an extended octadecyl alkane chain. The calibration curves of xerogels systems with varying R group chain length shows increasing sensitivity (slope) with increasing chain length, from methyl (**1a**) to propyl (**1b**) and octyl (**1c**) before

linearity is severely lost with the octadecyl R group (**1d**). Additionally, the excellent linearity/step response of the curves for the smaller chain length systems remains high - all exhibited correlation coefficients (R^2) of ~0.999_4 with linear ranges extending from 0 to at least 20 mM. These results suggest that an increasing aliphatic character within the films is beneficial for sensitivity, at least to a point.

Figure 5B shows the calibration curves for layered-xerogel biosensors formed from silane derivatives with different functional groups at R (**2-6**) including thiol, hydroxyl, amino, isobutyl, and phenyl moieties. Here again, most of the results show high linear correlation (average R^2 of 0.999_2 overall) and step responses out to high glucose concentrations (e.g., 20-30 mM) and a functional group dependency on sensitivity. Xerogels from silane precursors with a hydroxyl (HMTES) or isobutyl (IBTMS) functionality at the R group were significantly more sensitive than films featuring amino (APTMS), thiol (MPTMS), or phenyl groups (PhTMS). We note that all of these films, varying in either chain length or functionality, resulted in well-defined

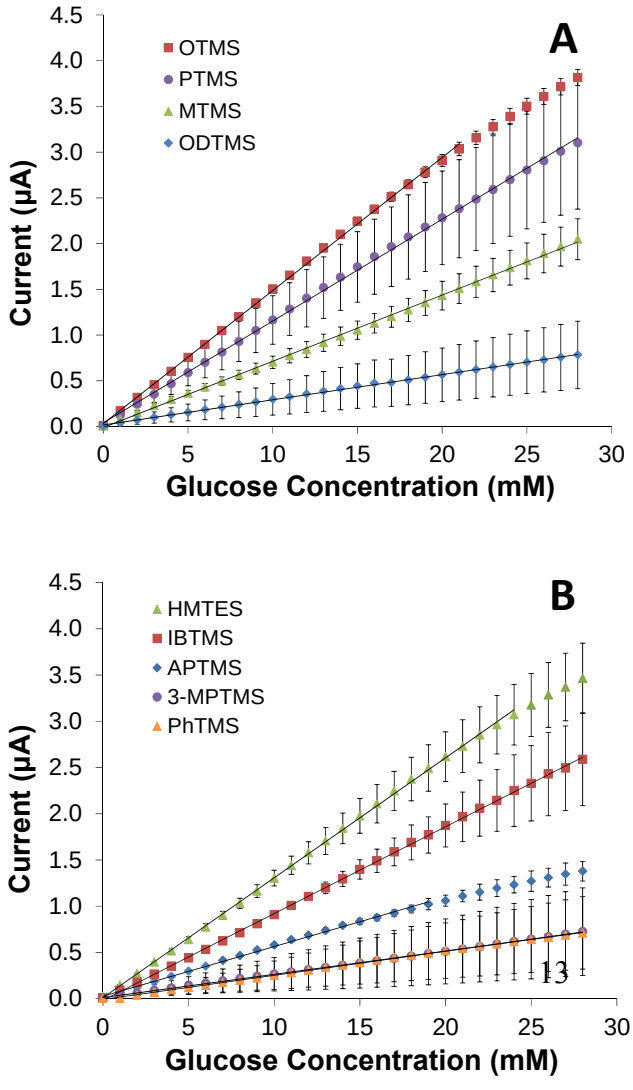

Figure 5. Calibration curves for layered xerogel glucose biosensors constructed with platinum electrodes modified with layers of xerogels formed from silane precursors that vary in **(A)** chain length or **(B)** functional group and capped with polyphenol and polyurethane. Linear regression is performed for linear step-responses (linear range). Note: In contrast to other films, well-defined steps were recorded for the entire range tested (no open symbols, Fig. 2).

step responses from 0 to 28 mM or beyond, shown as closed symbols in Fig. 5. Xerogels fabricated from 11-MUDTMS were also tested (not shown) but resulted in poor step-responses and ineffective calibration curves in line with what was observed for octadecyl xerogels during the chain length study. These findings establish a dependence on functional groups within the sol-gel matrix that house the enzyme. That relationship is consistent with a recent report by Montilla and coworkers[26] who showed that the electron transfer of cytochrome *c* encapsulated in a sol-gel was significantly influenced by the hydrophobicity of the gel's microenvironment, a property manipulated by using silanes with different terminal groups.

Sensing performance testing of the more successful xerogel systems from the aforementioned chain length/functional group study (i.e., OTMS, HMTES, IBTMS), those with sufficient sensitivity for development as a sensor, yielded the results summarized in **Table 1.** As with the featured PTMS-layered xerogel system (Fig. 2B), the other xerogel layered systems that exhibited significant sensitivity all behaved similarly in control experiments that tested the system performance at various stages of the L-B-L assembly. That is, systems lacking either the PP and/or PU layers (i.e., only doped and undoped xerogel layers) showed a limited step response toward increasing concentrations of glucose. Systems without the PU, PP, and diffusional, undoped xerogel layer (i.e., only enzyme-doped xerogel at the platinum electrode) resulted in high sensitivity and usable signal only for concentrations $\leq$ 5 mM. I-*t* curves and corresponding calibration curve comparisons are provided in the Supporting Information for OTMS, HMTES, and IBTMS. Each of these systems yielding significant glucose sensitivity was also tested for interferent responses. Interestingly, all three of these systems drastically outperform the previously presented PTMS system in terms of inteferent response analysis. Interferent I-*t* curves as well as selectivity coefficient values/tracking initially and over the span of a two-week period indicate the strength of OTMS, HMTES and IBTMS in this regard while they also maintain greater sensitivity toward glucose compared to PTMS system (Fig.2). During the two-week stability tests, the initial effective selectivity coefficients for common interferents were generally stable with only a very modest initial increase for acetaminophen selectivity after 48 hours and some erratic, though still largely blocked, behavior observed for uric acid. HMTES

systems were the most stable of the group with IBTMS exhibiting the most variability (Supporting Information). In essence, however, all of the systems were effective at discriminating against acetaminophen, a difficult interferent that is critically important to control for clinical applications of sensors. Additionally, the stability (i.e., response time and sensitivity) of these systems was found to be similar to that of PTMS over the course of two weeks. Control experiments again established that a specific combination of L-B-L fabrication is required for effective performance. That is, the extended linear range of defined step-like responses and the effective discrimination against interferents was only achieved with specific L-B-L construction that allows the composite of materials to work in concert with each other (Supporting Information). Additionally, rather than sandwiched in between the PU and xerogel, PP was applied before the formation of the xerogel layers and resulted in some systems (e.g., IBTMS, MPTMS) exhibiting larger selectivity coefficients (i.e., less selectivity) for certain interferents like acetaminophen (results not shown).

The significant difference in sensitivity between the various types of xerogel films prompted exploration of film xerogel permeability/porosity as a function of silane precursor. While the difficulty of completely separating these two film properites is openly acknowledged, experiments were conducted under the assumption that permeability would be predominantly be a function of interface hydrophobicity with porosity more dependent on film structure. The xerogel porosity/permeability was evaluated using multiple methods: H_2O_2 permeability, redox probe molecule voltammetry, and contact angle goniometry (CAG). Additionally, the porosity of certain films was assessed with rudimentary methylene blue dye adsorption designed for sol-gel analysis[27] as well as SEM imaging. The collective results from porosity/permeability assessement experiments are primarily summarized in **Table 2** (see Supporting Information for SEM images) and collectively promote enough general agreement to establish relative xerogel permeability/porosity. Overall, the work suggests that sensor sensitivity dependence on silane precursor structure may be related to the permeability/porosity of the xerogel materials.

Given its role in the enzymatic reaction and sensing scheme (Fig. 1), H_2O_2 permeability, determined via the ratio of H_2O_2 oxidative current at the xerogel compared

to a bare electrode, is critical to film functionality and was employed as a baseline measure of xerogel permeability.[16,17] Even moderately small pores should allow for peroxide penetration to the electrode interface. **Table 2** shows the oxidative current observed during 1 mM injections of H_2O_2 at various xerogel films and bare platinum. Table 2 orders the xerogels from least (MUDTMS) to most (OTMS) H_2O_2 permeability. The most sensitive films for glucose biosensing (i.e., OTMS, HMTES, PTMS, and IBTMS) all display substantial H_2O_2 oxidation current, suggesting that H_2O_2 permeability is indeed critical.

Cyclic voltammetry of a panel of solution redox probe molecules at the xerogel interfaces was used to assess film hydrophobicity and its effect on diffusional species. An important aspect of a sensing mechanism is its dependence on glucose diffusion from solution into the films. More specifically, the voltammetry of anionic potassium ferricyanide ($K_3Fe(CN)_6$), cationic ruthenium hexamine ($Ru(NH_3)_6Cl_3$), and neutral hydroxymethyl ferrocene (HMFc) at the various xerogel interfaces was recorded. **Figure 6** displays example voltammograms from $K_3Fe(CN)_6$ experiments that represent the different categories used to describe the voltammetry response of each of the three redox probes (**Table 2**) including diffusional, partially blocked/diffusional, partially blocked, and completely blocked behaviors. The prevailing thought behind these experiments is more hydrophobic films, xerogels with higher contact angles, will be more efficient at blocking the approach and electron transfer of charged solution molecules ($K_3Fe(CN)_6$ and $Ru(NH_3)_6Cl_3$) while the neutral HMFc probe will be more sensitive to electrode access sites in hydrophobic films. As expected, the charged probes behaved similarly to each other at the majority of the xerogels (see Table 2). Interestingly, however, charged redox probe voltammetry at the four most effective films, in conjunction with measured contact angles, yield little correlation between blocking and hydrophobicity. That is, the most glucose sensitive systems, IBTMS, PTMS, HMTES, and OTMS, exhibited average CAs of 79.2°, 88.3°, 62.6°, and 93.1°, respectively, a mixture of hydrophobic (i.e., larger CAs) and hydrophilic (i.e., smaller CAs) films. HMTES and OTMS, the two films with the highest sensitivity toward glucose, 0.1141 and 0.1671 μA/mM, respectively, display contact angles 30° apart, a substantial difference in hydrophobic character.

A neutral probe molecule, HMFc should be more sensitive at hydrophobic interface than the charged probes. HMFc voltammetry descriptors are included in **Table 2** with voltammograms in Supporting Information. As expected, HMFc displayed more diffusional behavior at the more hydrophobic films (e.g., IBTMS, APTMS, ODTMS) and was blocked more at the less hydrophobic films (e.g., MUDTMS, MPTMS, MTMS) compared to the charged probes. If the four most successful films are examined, all four show some level of diffusional voltammetry for HMFc.

Results suggest that the most successful sensing xerogels exhibit high H_2O_2 permeability as well as diffusional voltammetry for all three redox probes, regardless of the probe's charged state and in spite of vastly different hydrophobic character as measured by CAG. For example, OTMS xerogel exhibits the highest contact angle (i.e., highest hydrophobic character at 93.1°), yet promotes diffusional electrochemistry for all three probe molecules and the largest H_2O_2 permeability. Representative SEM images of the different films show that the more effective xerogels seem to possess more obvious porosity as well that correlates with diffusional redox probe behavior and that images of blocked films appear relatively featureless and uniform (see Supporting Information).[22] Taken collectively, these results seem to suggest that porosity, rather than hydrophobic character, may be the primary influence on sensor performance/sensitivity. The results, however, are not conclusive and hydrophobic effects cannot be completely discounted. Certain anomalies, while repeatable, cannot be easily explained. APTMS xerogels, for example, one of the more hydrophobic systems according to CAG (86.7°), exhibited high H_2O_2 permeability, diffusional behavior for charged probes and partially blocked HMFc voltammetry, but did not perform well as sensing material (Fig. 5B) even though these properties are similar to high performing OTMS xerogels.

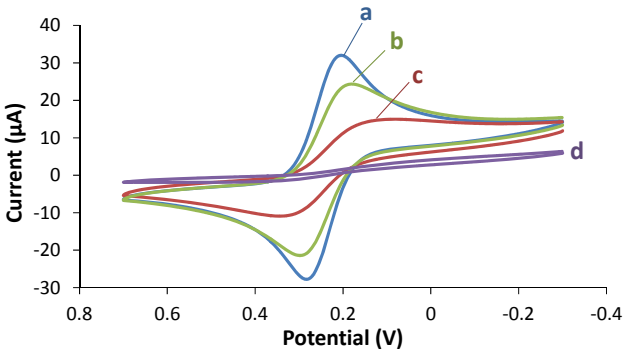

Figure 6. Cyclic voltammetry of anionic 5 mM $K_3Fe(CN)_6$ in 0.5 M KCl at platinum electrodes modified with xerogels formed from different silanes that illustrate four classifications designated in Table 2 to describe xerogel permeability/porosity. In these examples, the voltammetry descriptors are **(a)** diffusional (e.g., OTMS), **(b)** partially blocked/diffusional (e.g., PTMS), **(c)** partially blocked (e.g., IBTMS), or **(d)** blocked (e.g., MPTMS). Similar criteria were applied when describing the voltammetry of cationic and neutral redox probes, 2.5 mM $Ru(NH_3)_6Cl_3$ in 0.1 M KNO_3 and 1 mM hydroxymethyl ferrocene (HMFc) in 0.1 M $HClO_4$, respectively (see Table 2). Note: $K_3Fe(CN)_6$ and $Ru(NH_3)_6Cl_3$ voltammetry was recorded at 100 mV/sec and HMFc at 25 mV/sec.

■ CONCLUSIONS

Rational design of a multi-layer interface for 1st generation glucose biosensing has been demonstrated. Each layer within the scheme serves a specific purpose, including a xerogel layer housing the enzymatic reaction and acting as a signal transducer as well as a xerogel layer functioning to control diffusion of both glucose and O_2 to the enzyme-doped layer. Capping layers of electropolymerized polyphenol layers and a polyurethane blended layer work to effectively eliminate the approach and redox activity of common interferents including some of the more challenging species like acetaminophen and ascorbic acid. The L-B-L approach in this study results in an extended step responses that translate into dramatic linear/dynamic ranges. The specificity of the combination of the four layers and the ability to systematically alter their selectivity via the structure of the xerogel's silane precursor and the subsequent porosity of the formed gel suggests that the significance of this strategy may be its adaptability to other analytes of interest including targets for real-time continuous monitoring in clinical settings.[1,28]

■ Supporting Information

Amperometric I-*t* curves, stability results, and/or calibration curves for control experiments and interferent experiments for OTMS, HMTES, and IBTMS xerogel systems. SEM images of various xerogel films. Amperometric I-*t* for inteferent species at different thicknesses of polyphenol membranes including comparisons of selectivity coefficients at various assembly stages. Comparison of sensor performance to literature values.

■ AUTHOR INFORMATION

Corresponding Author

*Email: mleopold@richmond.edu

Notes:

The authors declare no competing financial interest.

■ ACKNOWLEDGEMENTS

This research was generously supported by funding from Virginia's Commonwealth Health Research Board and the National Science Foundation (CHE-1401593), the Floyd D. and Elisabeth S. Gottwald Endowment, as well as student fellowships from the University of Richmond's Undergraduate Research Committee and Chemistry Department Puryear-Topham-Gupton-Pierce Fund (NGP). We would like to thank Luke T. DiPasquale and Tram Anh Bui for their important contributions to this work. We gratefully acknowledge the following people for making research possible at the University of Richmond: Drs. T. Leopold, R. Kanters, D. Kellogg, R. Miller, and W. Case, as well as Christie Davis (Director of Microscopy, Department of Biology), Russ Collins, Phil Joseph, Mandy Mallory, and Lamont Cheatham. A very personal note of thanks is given to my mentors, Professors Edmond F. Bowden and Royce W. Murray, for their support and guidance.

References

(1) Wang, J. Electrochemical Glucose Biosensors. *Chem. Rev.* **2008**, *108*, 814-825.

(2) Pohanka, M.; Skládal, P. Electrochemical Biosensors -- Principles and Applications. *Journal of Applied Biomedicine* **2008**, *6*, 57-64.

(3) Kerman, K.; Saito, M.; Tamiya, E.; Yamamura, S.; Takamura, Y. Nanomaterial-Based Electrochemical Biosensors for Medical Applications. *TrAC, Trends Anal. Chem.* **2008**, *27*, 585-592.

(4) Ciobanu, M.; Taylor, D. E., Jr.; Wilburn, J. P.; Cliffel, D. E. Glucose and Lactate Biosensors for Scanning Electrochemical Microscopy Imaging of Single Live Cells. *Anal.Chem.* **2008**, *80*, 2717-2727.

(5) Patel, J.; Radhakrishnan, L.; Zhao, B.; Uppalapati, B.; Daniels, R. C.; Ward, K. R.; Collinson, M. M. Electrochemical Properties of Nanostructured Porous Gold Electrodes in Biofouling Solutions. *Anal. Chem.* **2013**, *85*, 11610-11618.

(6) Romero, M. R.; Garay, F.; Baruzzi, A. M. Design and Optimization of a Lactate Amperometric Biosensor Based on Lactate Oxidase Cross-Linked with Polymeric Matrixes. *Sens. Actuators, B* **2008**, *B131*, 590-595.

(7) Rubio-Retama, J.; Lopez-Cabarcos, E.; Lopez-Ruiz, B. High Stability Amperometric Biosensor Based on Enzyme Entrapment in Microgels. *Talanta* **2005**, *68*, 99-107.

(8) Bowden, E. F.; Clark, R. A.; Willit, J. L.; Song, S. Protein Monolayer Electrochemistry: A Strategy for Probing Biological Electron Transfer Kinetics. *Proceedings - Electrochemical Society* **1993**, *93-11*, 34-45.

(9) Loftus, A. F.; Reighard, K. P.; Kapourales, S. A.; Leopold, M. C. Monolayer-Protected Nanoparticle Film Assemblies as Platforms for Controlling Interfacial and Adsorption Properties in Protein Monolayer Electrochemistry. *J. Am. Chem. Soc.* **2008**, *130*, 1649-1661.

(10) Walcarius, A.; Mandler, D.; Cox, J. A.; Collinson, M.; Lev, O. Exciting New Directions in the Intersection of Functionalized Sol-Gel Materials with Electrochemistry. *J. Mater. Chem.* **2005**, *15*, 3663-3689.

(11) Narang, U.; Prasad, P. N.; Bright, F. V.; Ramanathan, K.; Kumar, N. D.; Malhotra, B. D.; Kamalasanan, M. N.; Chandra, S. Glucose Biosensor Based on a Sol-Gel-Derived Platform. *Anal. Chem.* **1994**, *66*, 3139-3144.

(12) Pandey, P. C.; Upadhyay, S.; Pathak, H. C. A New Glucose Biosensor Based on Sandwich Configuration of Organically Modified Sol-Gel Glass. *Electroanalysis* **1998**, *11*, 59.

(13) Pandey, P. C.; Upadhyay, S.; Pathak, H. C.; Tiwari, I.; Tripathi, V. S. Studies on Glucose Biosensors Based on Nonmediated and Mediated Electrochemical Oxidation of Reduced Glucose Oxidase Encapsulated within Organically Modified Sol-Gel Glasses. *Electroanalysis* **1999**, *11*, 1251.

(14) Sekretaryova, A. N.; Beni, V.; Eriksson, M.; Karyakin, A. A.; Turner, A. P.; Vagin, M. Y. Cholesterol Self-Powered Biosensor. *Anal. Chem.* **2014**, *86*, 9540-9547.

(15) Yashina, E. I.; Borisova, A. V.; Karyakina, E. E.; Shchegolikhina, O. I.; Vagin, M. Y.; Sakharov, D. A.; Tonevitsky, A. G.; Karyakin, A. A. Solâ^'Gel Immobilization of Lactate Oxidase from Organic Solvent: Toward the Advanced Lactate Biosensor. *Anal. Chem.* **2010**, *82*, 1601-1604.

(16) Koh, A.; Lu, Y.; Schoenfisch, M. H. Fabrication of Nitric Oxide-Releasing Porous Polyurethane Membranes-Coated Needle-Type Implantable Glucose Biosensors. *Anal. Chem.* **2013**.

(17) Soto, R. J.; Privett, B. J.; Schoenfisch, M. H. In Vivo Analytical Performance of Nitric Oxide-Releasing Glucose Biosensors. *Anal. Chem.* **2014**, *86*, 7141-7149.

(18) Guo, S.; Dong, S. Biomolecule-Nanoparticle Hybrids for Electrochemical Biosensors. *TrAC Trends in Analytical Chemistry* **2009**, *28*, 96-109.

(19) Pandey, P.; Datta, M.; Malhotra, B. D. Prospects of Nanomaterials in Biosensors. *Anal. Lett.* **2008**, *41*, 159-209.

(20) Wang, Z.; Luo, X.; Wan, Q.; Wu, K.; Yang, N. A Versatile Matrix for Constructing Enzyme-Based Biosensors. *ACS Applied Materials & Interfaces* **2014**, *6*, 17296-17305.

(21) Salimi, A.; Compton, R. G.; Hallaj, R. Glucose Biosensor Prepared by Glucose Oxidase Encapsulated Sol-Gel and Carbon-Nanotube-Modified Basal Plane Pyrolytic Graphite Electrode. *Anal. Biochem.* **2004**, *333*, 49-56.

(22) Freeman, M. H.; Hall, J. R.; Leopold, M. C. Monolayer-Protected Nanoparticle Doped Xerogels as Functional Components of Amperometric Glucose Biosensors. *Anal. Chem.* **2013**, *85*, 4057-4065.

(23) Chen, X.; Hu, Y.; Wilson, G. S. Glucose Microbiosensor Based on Alumina sol–gel matrix/electropolymerized Composite Membrane. *Biosensors and Bioelectronics* **2002**, *17*, 1005-1013.

(24) Bartlett, P. A Review of the Immobilization of Enzymes in Electropolymerized Films. *J. Electroanal. Chem.* **1993**, *362*, 1.

(25) Sánchez-Obrero, G.; Cano, M.; Ávila, J. L.; Mayén, M.; Mena, M. L.; Pingarrón, J. M.; Rodríguez-Amaro, R. A Gold Nanoparticle-Modified PVC/TTF-TCNQ Composite Amperometric Biosensor for Glucose Determination. *J Electroanal Chem* **2009**, *634*, 59-63.

(26) Gamero-Quijano, A.; Huerta, F.; Morallon, E.; Montilla, F. Modulation of the Silica Sol-Gel Composition for the Promotion of Direct Electron Transfer to Encapsulated Cytochrome c. *Langmuir* **2014**, *30*, 10531-10538.

(27) Harris, T.; Knobbe, E. Assessment of Porosity in Sol-Gel Silica Thin Films by Dye Adsorption. *J. Mater. Sci. Lett.* **1996**, *15*, 153-155.

(28) Kotanen, C. N.; Moussy, F. G.; Carrara, S.; Guiseppi-Elie, A. Implantable Enzyme Amperometric Biosensors. *Biosensors and Bioelectronics* **2012**, *35*, 14.

Table 1. Layered Xerogel-Based Amperometric Glucose Biosensor Performance

Xerogel Silane Precursor	n	Glucose Sensitivity (μA/mM)	Response Time ($t_{R-95\%}$) (s)	Linear Range† (mM)	Dynamic Range† (mM)	Limit of Detection‡ (μM)
Chain Length						
MTMS	3	0.0779 (±0.0005)	12.5 (±4.4)	28	28	12.4 (±0.4)
PTMS	3	0.0983 (±0.0007)	16.5 (±9.3)	>28	>28	18.1 (±2.2)
OTMS	2	0.1671 (±0.0014)	17.5 (±2.1)	21	28	18.8 (±0.02)
ODTMS	3	0.0275 (±0.0002)	10.3 (±6.8)	28	28	24.3 (±6.2)
R – Group						
MPTMS	3	0.0252 (±0.0001)	8.2 (±5.8)	>28	>28	89.8 (±28.7)
HMTES	2	0.1141 (±0.0010)	27.0 (±2.8)	24	28	8.2 (±3.5)
IBTMS	2	0.0939 (±0.0009)	20.5 (±12.0)	25	28	21.5 (±6.2)
APTMS	3	0.0686 (±0.0007)	25.0 (±1.4)	19	28	18.5 (±8.7)
PhTMS	3	0.0261 (±0.0001)	19.3 (±3.1)	28	28	49.6 (±26.3)

Notes: †Typical values with some exceeding 28 mM and not recorded.
‡ Limit of detection determined from $3\sigma_{blank}/b_1$ method.

Table 2. Porosity, Permeability, and Hydrophobicity Assessment of Xerogels Formed From Various Silane Precursors

Silane Precursor	**Structure** (Scheme I)	**i_a (H_2O_2)**[w] (nA)	**Surface Area**[x] (m^2/g)	**$K_3Fe(CN)_6$**[y] (5 mM)	**$Ru(NH_3)_6Cl_3$**[y] (2.5 mM)	**HMFc**[y] (1 mM)	**Contact Angle**[z]
MUDTMS	(2)	-0.042 (±0.072) n=3	-	Blocked	Blocked	Blocked	68.1 (±0.2) n=2
PhTMS	4	0.47 (±0.30) n=3	-	Blocked	Blocked	-	68.4 (±0.1) n=2
MPTMS	2	1.931 (±2.078) n=15	114 (±65) n=2	Blocked [d]	Blocked	Blocked	60.4° (±1.5) n=2
ODTMS	1d	16.87 (±12.54) n=8	-	Blocked	Partially Blocked	Diffusional	79.8° (±3.4) n=2
IBTMS	3	129.8 (±39.3) n=7	-	Partially Blocked [c]	Partially Blocked/Diffusional	Diffusional	79.2 (±2.0) n=2
MTMS	1a	320.7 (±64.9) n=8	246 (±1) n=2	Partially Blocked	Partially Blocked	Blocked	59.8 (±6.0) n=2
PTMS	1b	289.0 (±290.2) n=9	-	Partially Blocked/ Diffusional [b]	Diffusional	Blocked	88.3° (±1.7) n=3
HMTES	6	998.2 (±86.7) n=3	-	Partially Blocked/ Diffusional	Partially Blocked/Diffusional	Partially Blocked/ Diffusional	62.6 (±0.3) n=2
APTMS	5	1026 (±287)n=3	-	Diffusional	Diffusional	Partially blocked	86.7 (±2.3) n=2
OTMS	1c	1481 (±602.7) n=9	-	Diffusional [a]	Diffusional	Diffusional	93.1° (±0.7) n=3
Platinum	-	2768 (±1487) n=12	-	Diffusional	Diffusional	Diffusional	-

Notes: [w] Determined from the amperometric response of 1 mM H_2O_2 injections at various xerogel films.
[x] Determined from methylene blue adsorption (Harris and Knobbe.)[27] Gas sorption isotherm analysis (Quantachrome Instruments) confirmed relative surface area of a random sample of different films (MPTMS, PTMS, and OTMS).
[y] Assessed via cyclic voltammetry of electrochemical probes molecules ($K_3Fe(CN)_6$, HMFc, or $Ru(NH_3)_6Cl_3$) displaying more diffusional or blocked behavior[a-d] as defined in Figure 6 with examples **a-d** for $K_3Fe(CN)_6$.
[z] Contact angles measured on 10 µL drops after deposition of xerogel on glass slides, 48 hour aging in controlled humidity (50% R.H).

Graphical Abstract